Electronic Supplementary Information

Interwoven MnO/Co-Derived N-Doped Carbon Nanotube Composites as Highly Efficient and Durable Bifunctional Oxygen Catalysts for Zinc-Air Batteries

Yun Yang‡ [1], Qing Long‡ [2], Wei Wang * [2], Junlin Huang * [2], Yufei Zhao [3, 4], Hao Liu [4], Hong Gao * [3]

[1] *College of Chemistry and Environmental Engineering, Shiyan Key Laboratory of Biological Resources and Eco-environmental Protection, Hanjiang Normal University, Shiyan, Hubei 442000, China*

[2] *Key Laboratory of Hunan Province for Advanced Carbon-based Functional Materials, Hunan Institute of Science and Technology, Yueyang 414006, P. R. China*

[3] *Joint International Laboratory on Environmental and Energy Frontier Materials, School of Environmental and Chemical Engineering, Shanghai University, Shanghai 200444, China.*

[4] *Centre for Clean Energy Technology, University of Technology Sydney, Broadway, Sydney, NSW 2007, Australia.*

‡ These authors contributed equally to this work.

***Corresponding authors**

E-mail addresses: ww1454174@foxmail.com (Wei Wang), junlinhuang1022@163.com (Junlin Huang), hgao1122@shu.edu.cn (Hong Gao).

Structural Characterization

The sample's Powder X-ray diffraction (XRD) patterns were collected with Cu Kα radiation on a Philips X'pert X-ray diffractometer. The morphology and structural characteristics were examined using scanning electron microscopy (SEM, ZEISS Sigma 300), transmission electron microscopy (TEM, FEITF 20), and high-resolution transmission electron microscopy (HRTEM, FEITF 20). X-ray photoelectron spectroscopy (XPS, Thermo Scientific K-Alpha) was utilized for additional surface composition analysis. Thermal gravimetric analysis (TGA) was performed in air using a PerkinElmer STA-8000 thermal analyzer within the temperature range of 30 °C to 800 °C at a heating rate of 10 °C min^{-1}. Raman spectra were obtained using a Raman spectrometer (DXRxi). The specific surface area was determined through N_2 adsorption/desorption analysis at 77 K using a Micromeritics ASAP 2020 HD analyzer.

Koutecky-Levich equation

In the calculation of the number of transferred electrons (n) for each oxygen molecule during the ORR process, the Koutecky-Levich equation utilizes the slope of the best linear fitting line.

$$\frac{1}{J}=\frac{1}{J_L}+\frac{1}{J_K}=\frac{1}{Bw^{1/2}}+\frac{1}{J_K} \quad (1)$$

$$B=0.2nFC_0(D_0)^{2/3}v^{-1/6} \quad (2)$$

Where J (mA cm^{-2}) is the measured current density, J_K (mA cm^{-2}) and J_L (mA cm^{-2}) denote the kinetic and diffusion-limiting current densities respectively, ω is the electrode rotation rate (rpm), n is the electron transfer number in oxygen reduction, F is the Faraday constant (F=96485C mol^{-1}), C_0 is the bulk concentration of O_2 (C_0=1.2×10^{-6} mol cm^{-3}), D_0 is the diffusion coefficient of O_2 (1.93 × 10^{-5} cm^2 s^{-1}), ν is the kinematic viscosity of the electrolyte (0.01 cm^2 s^{-1}), The constant 0.2 is adopted when the rotating speed is in rpm.

Randles-Sevcik equation

To compare the apparent diffusion coefficients (D) of O_2 during the ORR process for each sample, linear fitting was performed using the Randles-Sevcik equation:

$$i_p = (2.69 \times 10^5) n^{3/2} S D^{1/2} C v^{1/2} \quad (3)$$

where n is the number of electrons transferred, i_p is the peak current, S is the electrode area, D is the apparent diffusion coefficient of O_2, C is the saturated concentration of O_2, and v is the scan rate.

Electrochemical surface area measurements

The ECSA was determined using the C_{dl}, which is obtained from the capacitive current in the non-Faradaic region (1.18 to 1.28 V vs. RHE) measured by CV at different scan rates (1, 2, 3, 4, and 5 mV s^{-1}). By plotting the differences in current density (J_a-J_c) at 1.23 V (vs. RHE) against the scan rate, a linear slope is obtained, which is equal to twice the C_{dl}.

Zn-Air battery measurements

The solid zinc-air battery was constructed using a carbon cloth (2 cm × 2.5 cm) loaded with a catalyst (1 mg cm^{-2}) as the cathode, and a polished zinc sheet as the anode. The electrolyte contained 11.25 M KOH gel with the addition of 0.25 M ZnO. The battery underwent testing using the LAND and CHI electrochemical workstations.

For the liquid zinc-air battery tests, a homemade battery was used with a zinc plate (3 cm × 8 cm) as the anode. The air-electrode was created by drop-casting a catalyst ink (9 mg mL^{-1}) onto carbon paper (3 cm × 3 cm) with a copper-foam current collector. The zinc-air battery was then assembled by filling the electrolyte (6 M KOH and 0.2 M $Zn(Ac)_2$) between the anode and air-cathode.

Figure and captions

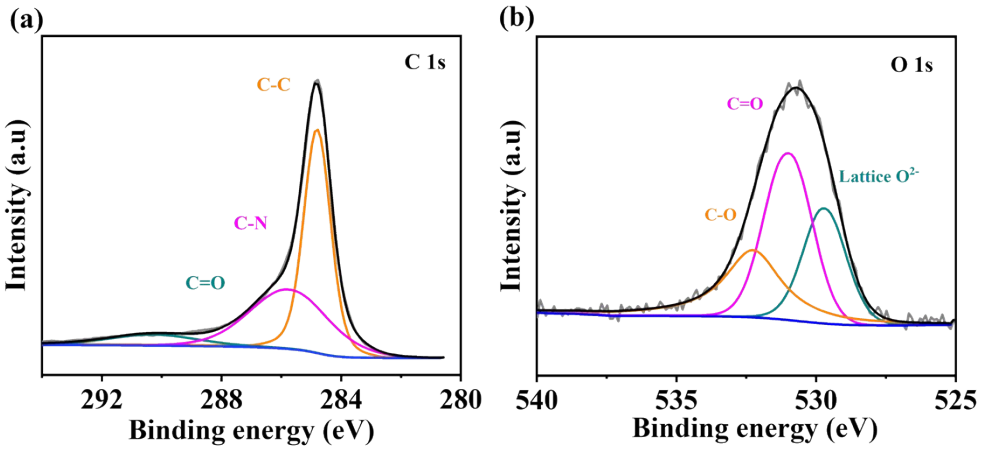

Fig. S1 High-resolution spectra of (a) C1s (b) O1s for MnO/Co-N-CNTs-750.

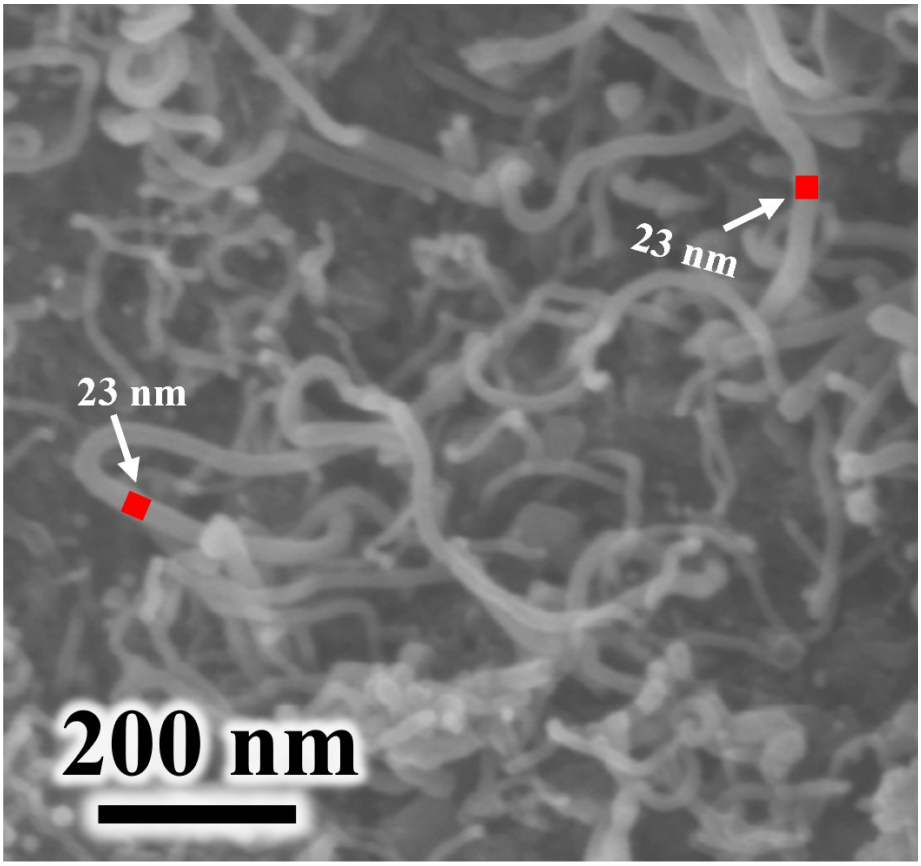

Fig. S2 SEM of MnO/Co-N-CNTs-750 and Nanotube Diameter.

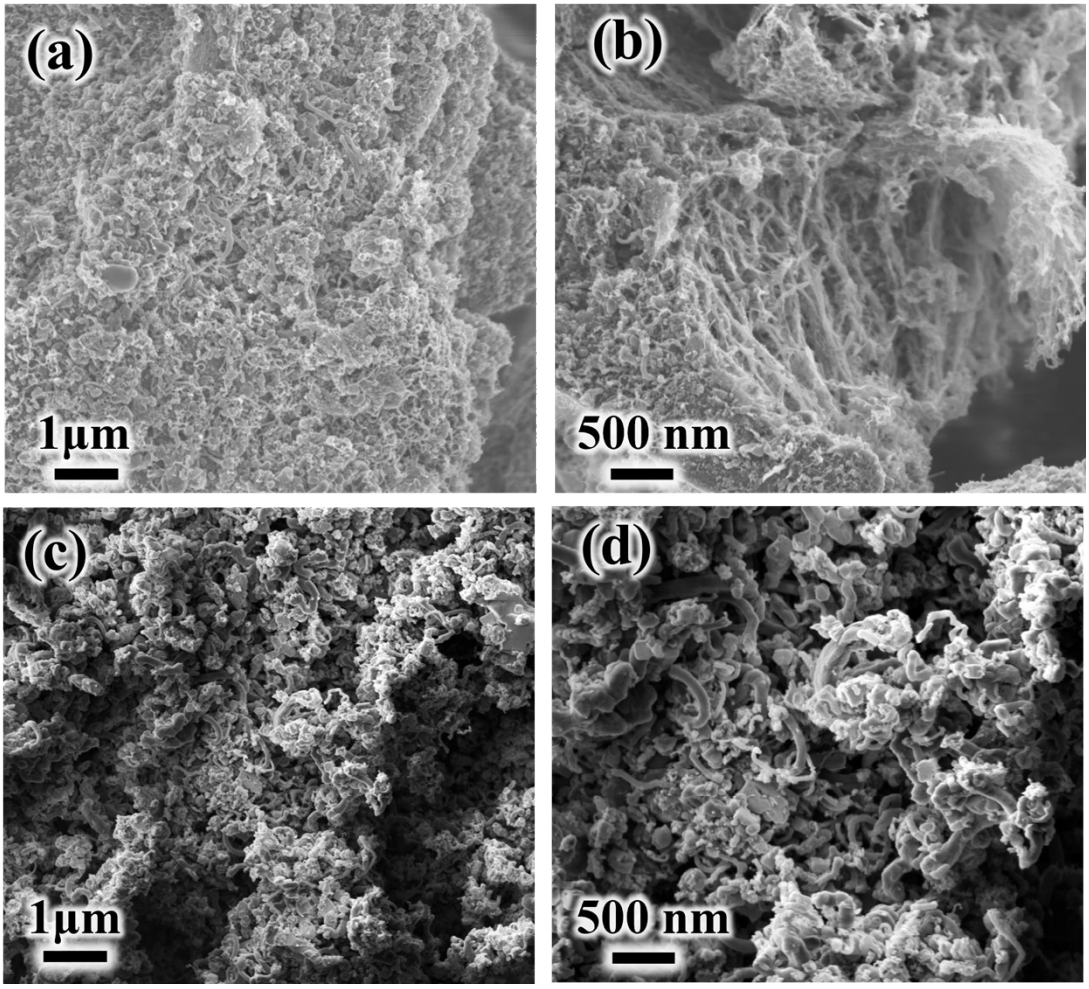

Fig. S3 SEM of (a,b) MnO/Co-N-CNTs-650,(c,d) MnO/Co-N-CNTs-850.

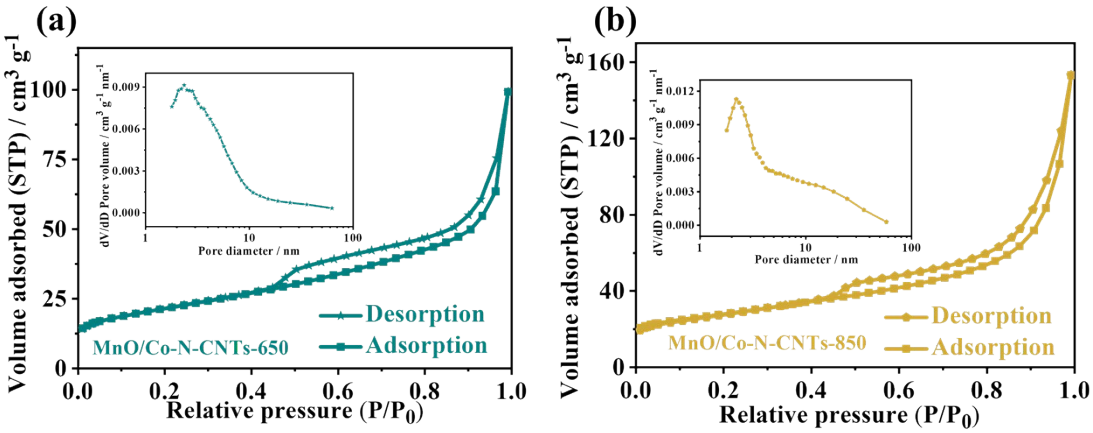

Fig. S4 N_2 adsorption/desorption isotherms and pore size distribution curves (the insert picture) of the (a) MnO/Co-N-CNTs-650 and (b) MnO/Co-N-CNTs-850.

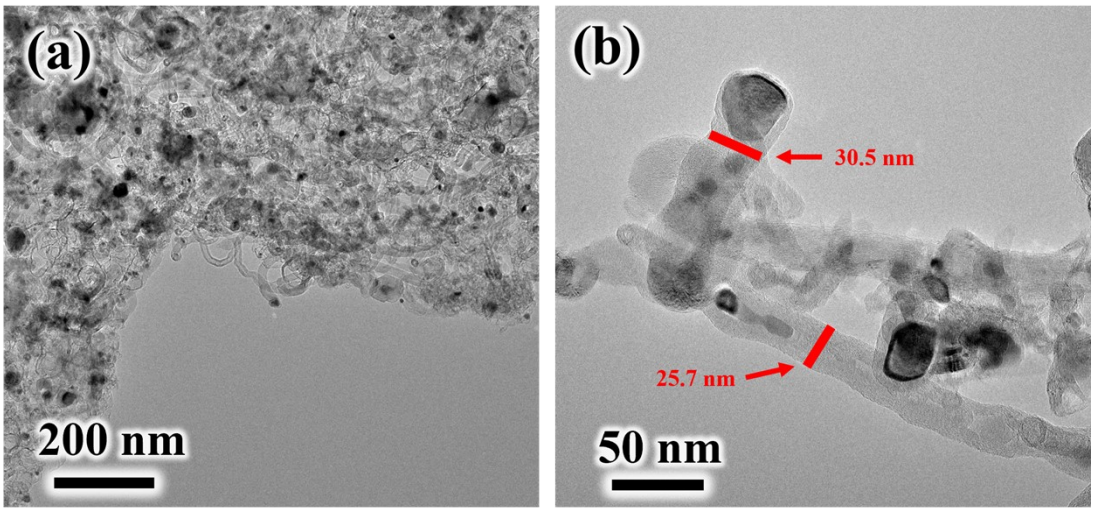

Fig. S5 (a,b) TEM images of MnO/Co-N-CNTs-750 and Nanotube Diameter.

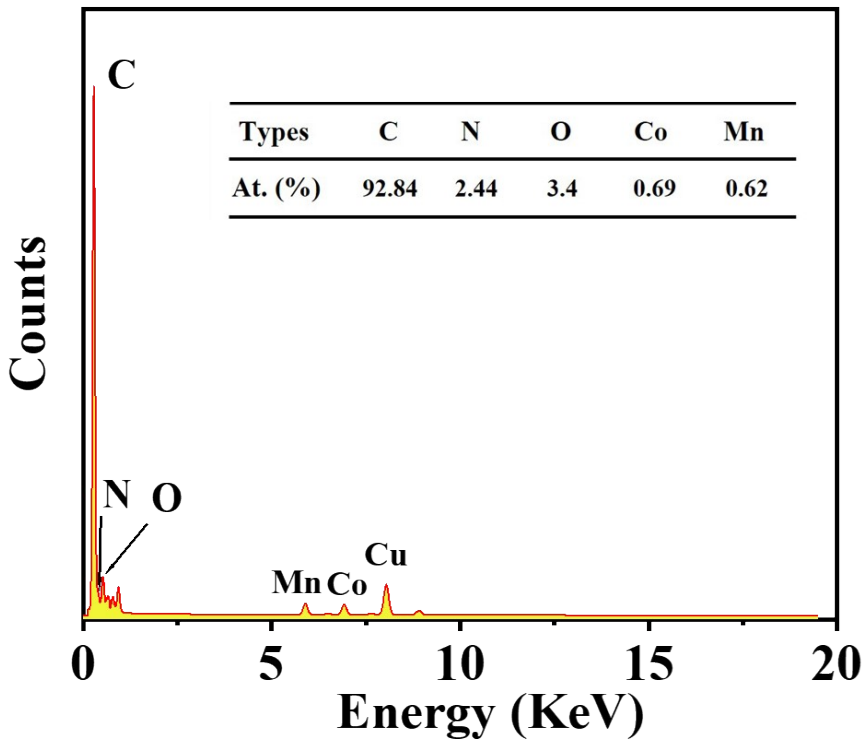

Types	C	N	O	Co	Mn
At. (%)	92.84	2.44	3.4	0.69	0.62

Fig. S6 EDS images of MnO/Co-N-CNTs-750 and Nanotube Diameter.

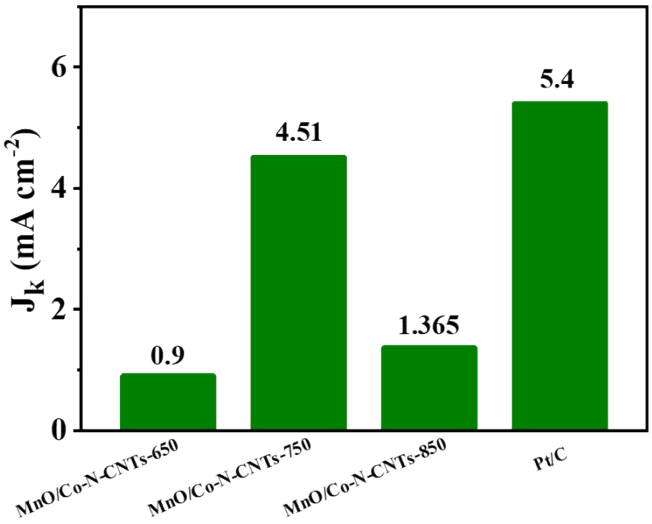

Fig. S7 J_K of MnO/Co-N-CNTs-650, MnO/Co-N-CNTs-750, MnO/Co-N-CNTs-850 and Pt/C at 0.82 Vvs.RHE.

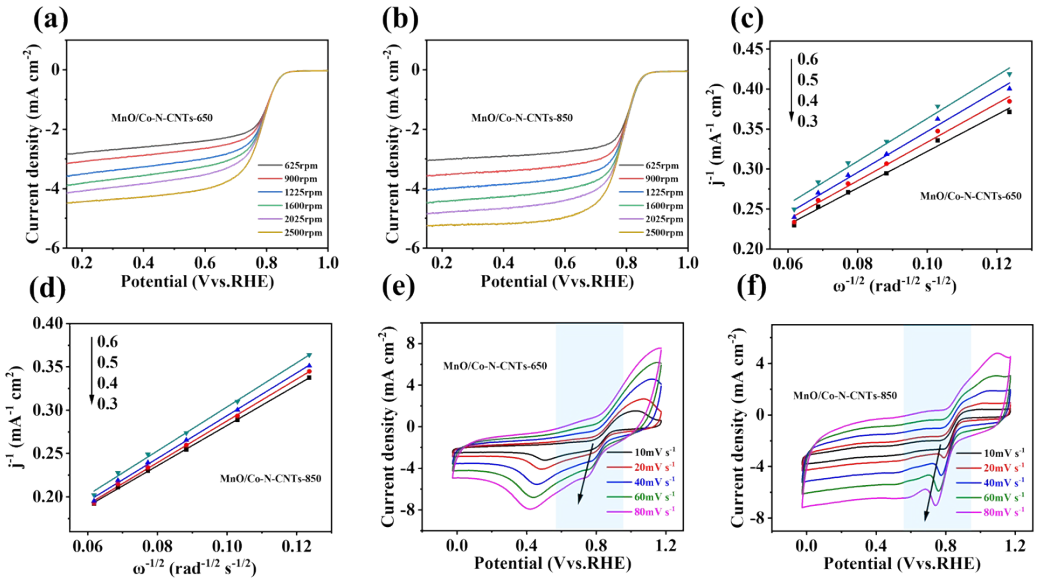

Fig. S8 The LSVs of of (a) MnO/Co-N-CNTs-650, (b) MnO/Co-N-CNTs-850 at different rotation rates. The K-L plots of (c) MnO/Co-N-CNTs-650, (d) MnO/Co-N-CNTs-850. CV curves on (e) MnO/Co-N-CNTs-650, (f) MnO/Co-N-CNTs-850 electrodes at various scan rates.

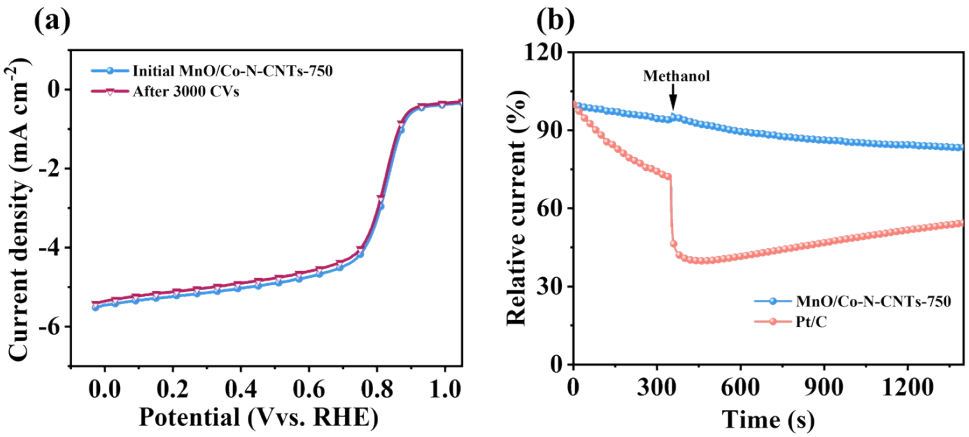

Fig. S9 (a) ORR LSV curves of MnO/Co-N-CNTs-750 before and after 3000 CVs. (b) Methanol tolerance tests of MnO/Co-N-CNTs-750 and Pt/C.

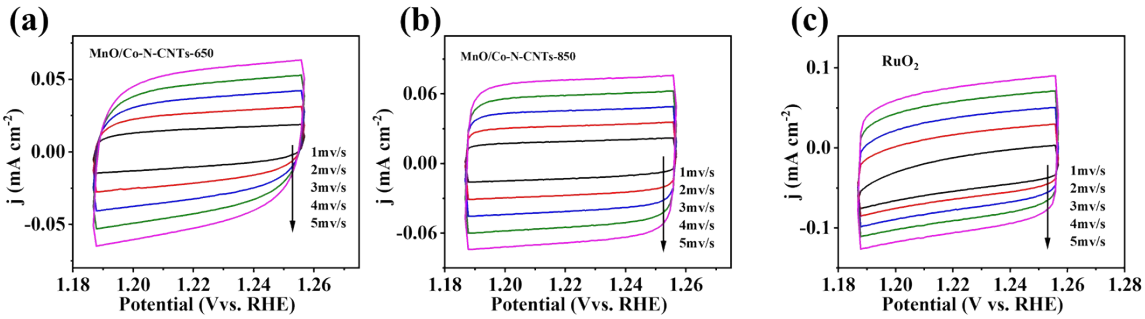

Fig. S10 Cyclic voltammograms (CVs) of (a) MnO/Co-N-CNTs-650, (b) MnO/Co-N-CNTs-850, (c) RuO_2.

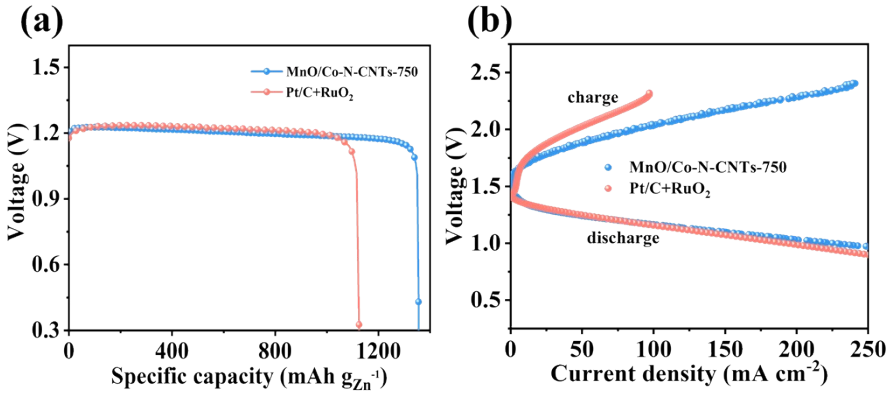

Fig. S11 (a) Discharge curves of solid-state ZABs at 5 mA cm^{-2}. (b) Charge/discharge polarization curves of MnO/Co-N-CNTs-750 based liquid ZABs.

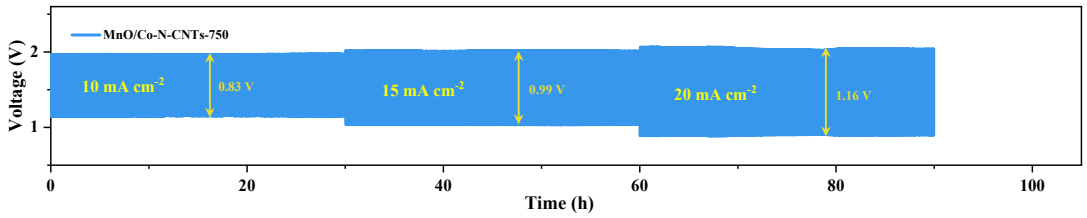

Fig. S12 Long cycle performance graph of MnO/Co-N-CNTs-750 at different current densities.

Table S1 The statistics of oxygen reduction performance parameters of the materials prepared in this work.

Samples	$E_{1/2}$ (V)	E_{onset} (V)	J_i (mA cm^{-2})
MnO/Co-N-CNTs-650	0.794	0.852	4.16
MnO/Co-N-CNTs-750	0.823	0.881	5.49
MnO/Co-N-CNTs-850	0.80	0.865	4.63
Pt/C	0.838	0.937	5.53